

Discriminating MSW solutions to the solar neutrino problem with flux-independent information at SuperKamiokande and SNO

G. L. Fogli, E. Lisi, and D. Montanino

Dipartimento di Fisica and Sezione INFN di Bari,

Via Amendola 173, I-70126 Bari, Italy

Abstract

The two possible Mikheyev-Smirnov-Wolfenstein (MSW) solutions of the solar neutrino problem (one at small and the other at large mixing angle), up to now tested mainly through absolute neutrino flux measurements, require flux-independent tests both for a decisive confirmation and for their discrimination. To this end, we perform a joint analysis of various flux-independent observables that can be measured at the SuperKamiokande and Sudbury Neutrino Observatory (SNO) experiments. In particular, we analyze the recent data collected at SuperKamiokande after 374 days of operation, work out the corresponding predictions for SNO, and study the interplay between SuperKamiokande and SNO observables. It is shown how, by using only flux-independent observables from SuperKamiokande and SNO, one can discriminate between the two MSW solutions and separate them from the no oscillation case.

PACS number(s): 26.65.+t, 13.15.+g, 14.60.Pq

The observed difference between experimental [1–5] and theoretical [6,7] absolute fluxes of solar neutrinos [8] can be explained by the Mikheyev-Smirnov-Wolfenstein (MSW) mechanism of matter-enhanced flavor oscillations of neutrinos [9]. Assuming for simplicity two-family oscillations, the MSW effect requires a neutrino square mass difference $\delta m^2 \sim 10^{-5}$ eV², the mixing amplitude in vacuum $\sin^2 2\theta$ being either small (~ 0.007) or large (~ 0.7) (see [10–13] for recent global analyses). The nuclear input uncertainties affecting the calculation of the absolute ν fluxes [8,14] make it desirable, however, to look also for flux-independent tests of the MSW effect for a definitive confirmation. Such tests can be performed in the new-generation, high-statistics solar ν experiments SuperKamiokande [5] and Sudbury Neutrino Observatory (SNO) [15].

In this work, we study the interplay among five flux-independent quantities measurable at SuperKamiokande and SNO, as listed in Table I. The first is the asymmetry between nighttime (N) and daytime (D) solar neutrino fluxes ($N - D/N + D$) at SuperKamiokande, which parametrizes possible time variations of the ν flux due to Earth matter effects (see [10] and references therein). The second is the fractional deviation of the average kinetic energy $\langle T \rangle$ of recoil electrons at SuperKamiokande ($\Delta\langle T \rangle/\langle T \rangle$), which parametrizes possible distortions of the neutrino energy spectrum due to oscillations [16,10,11]. The third and fourth observables are the analogous quantities ($N - D/N + D$ and $\Delta\langle T \rangle/\langle T \rangle$) for SNO. The fifth is the ratio of charged current (CC) to neutral current (NC) neutrino event rate in deuterium (CC/NC), which is peculiar to the SNO experiment (see [10,17] for recent analyses). None of these quantities depends on the absolute value of the ⁸B ν flux.

In order to study how the flux-independent observables can effectively help to test and discriminate the small (S) and large (L) mixing MSW solutions, we use as coordinates the observables themselves, rather than the usual mass-mixing parameters δm^2 and $\sin^2 2\theta$. In this way, the discriminative power of the SuperKamiokande and SNO experiments, as well as their interplay, can be shown and understood at glance.¹ In addition, we make use of the recent data collected from SuperKamiokande after 374 days of operation, which have been presented in several recent conferences [5,19–24].

Let us start with an update of the MSW fit to the neutrino rates measured by the Homestake [25], Kamiokande [2], SAGE [26], GALLEX [27], and SuperKamiokande (374 days) [5]. The most recent available data are compiled in Table II. The theoretical ingredients and the SuperKamiokande technical specifications (energy resolution and threshold) are taken as in [11]. In particular, the theoretical neutrino fluxes are taken from [6], the Earth regeneration effect is treated as in [10], and the experimental and theoretical uncertainties are included as in [14]. The results are shown in Fig. 1(a) in the plane of the oscillation parameters (for simplicity, we consider two neutrino families). The two familiar MSW solutions, one at small (S) and the other at large (L) mixing angle, are shown as allowed regions at 95% C.L. ($\Delta\chi^2 = 5.99$ for $N_{\text{DF}} = 2$). Notice that in Fig. 1(a) the fit includes *only* the total neutrino rates, i.e., only the flux-dependent information. The shapes of the S and L solutions can still change, to some extent, as this information is continually

¹ An analogous choice has been made in [18] to study the relation between *flux-dependent* observables at SuperKamiokande and SNO.

updated. However, they have proven to be quite stable. Therefore, it makes sense to use the flux-dependent solutions S and L as a guide to evaluate the likely expectations for the flux-independent observables, as we do in the following.

Next we consider the two SuperKamiokande observables $N - D/N + D$ and $\Delta\langle T\rangle/\langle T\rangle$. The night-day asymmetry measured in 374 days is [5]:

$$\begin{aligned} \frac{N - D}{N + D} \times 100 &= 3.1 \pm 2.4 \text{ (stat.)} \pm 1.4 \text{ (syst.)} \\ &= 3.1 \pm 2.8 \text{ (1}\sigma \text{ total)} , \end{aligned} \tag{1}$$

compatible with zero at $\sim 1\sigma$. We do not use here the additional SuperKamiokande information on nighttime rates in “fractions of nadir angle” [20], since they still have a low statistical significance and their systematics are not available at present.

The second SuperKamiokande flux-independent observable, namely, the deviation $\Delta\langle T\rangle/\langle T\rangle$ of the average (measured) electron kinetic energy from its standard value, can be obtained from the binned energy spectrum (after 374 days [5,24,28]) reported in Table III, by following the prescription described in the Appendix of Ref. [11]. The result is:

$$\begin{aligned} \frac{\Delta\langle T\rangle}{\langle T\rangle} \times 100 &= 0.95 \pm 0.62 \text{ (stat. + uncor. syst.)} \\ &\pm 0.30 \text{ (correl. syst.)} \\ &\pm 0.20 \text{ (}^8\text{B theor. shape)} \\ &\pm 0.12 \text{ (binning)} \\ &= 0.95 \pm 0.73 \text{ (1}\sigma \text{ total)} . \end{aligned} \tag{2}$$

In the above equation, the first error is due to statistics and to those systematics which are not correlated bin-by-bin (e.g., backgrounds). The second error is due to the those systematics that are fully correlated in each bin, the most important being the energy scale uncertainty [20,17]. The third error is due to the theoretical uncertainties in the shape of the ^8B neutrino spectrum [29]. Finally, the fourth uncertainty is due to the finite bin size [11] (it could be avoided if the value of $\Delta\langle T\rangle/\langle T\rangle$ were estimated directly from the raw data by the SuperKamiokande collaboration). From Eq. (2) we learn that: (i) there seems to be a slight ($\sim 1.3\sigma$) enhancement of the average electron energy, that might signal a distortion of the energy spectrum; (ii) at present, the largest error component is due to statistics plus uncorrelated systematics; and (iii) the ^8B ν spectrum uncertainty is nonnegligible.

In Fig. 1(b) the small (S) and large (L) mixing solutions of Fig. 1(a) are mapped in the plane spanned by the flux-independent SuperKamiokande observables $N - D/N + D$ and $\Delta\langle T\rangle/\langle T\rangle$. The small box with error bars represents the experimental data reported in Eqs. (1) and (2). Also shown for comparison are the older SuperKamiokande data (black dot with error bars) after 306 days of operation (see [11] and refs. therein), indicating a dramatic reduction of the electron energy uncertainty after 374 days, as a result of an improved energy calibration of the detector [20]. The two MSW solutions are well separated in the plane of Fig. 1(b). In fact, the small mixing solution predicts $\Delta\langle T\rangle/\langle T\rangle \simeq 0.8\text{--}1.4\%$ and $N - D/N + D \simeq 0\text{--}4\%$, while the large mixing solution corresponds to smaller values of $\Delta\langle T\rangle/\langle T\rangle$ (in the range $\pm 0.3\%$) and prefers relatively large values of $N - D/N + D$ (in the range $\simeq 2\text{--}17\%$).

From Fig. 1(b) it can be seen that the flux-independent SuperKamiokande data favor the small mixing solution, although the experimental uncertainties are not small enough yet to exclude either the large mixing solution or the no oscillation point [star in Fig. 1(b)]. Figure 1(b) also shows that, in order to discriminate the two MSW solutions between them and from the no oscillation scenario, the SuperKamiokande error bars should be reduced by a factor of two at least (which seems a reachable, although difficult, goal [20]). In particular, improvements in the experimental determination of $\Delta\langle T\rangle/\langle T\rangle$ appear decisive for separating the S and L solutions (assuming no significant changes in the experimental central values).

Next we study the relation between the SuperKamiokande and SNO flux-independent observables, which is the main goal of this work. For SNO we take the same prospective technical specifications as in [17,10]; in particular, we assume an electron kinetic energy threshold $T > 5$ MeV and 100% detection efficiency. With these assumptions, one has $(CC/NC)_0 = 1.88$ for no oscillation [17,10]; this number should be rescaled appropriately when the SNO efficiency will be measured.

Figure 2 shows SuperKamiokande vs. SNO flux-independent observables in various combinations. In each panel we map the two MSW solutions (S and L), as well as the no oscillation point (star). The solutions are well separated in the panels (a–d), while in the panels (e) and (f) there is some overlap. There is a high correlation between the expected values of $N - D/N + D$ in SuperKamiokande and SNO [Fig. 2(e)], which are approximately in a 1:2 ratio. Similarly, the $\Delta\langle T\rangle/\langle T\rangle$ values in Fig. 2(a) are highly correlated, with about the same proportionality factor. This means that, given a sufficiently precise measurement at SuperKamiokande *and* assuming the correctness of the MSW hypothesis, one can derive rather definite predictions for SNO.

As an application, we study the implication of the data in Eqs. (1) and (2), which, in Fig. 2, select the horizontal dotted bands at the the $\pm 1\sigma$ level. The corresponding predictions for SNO can be roughly obtained by projecting the part of the MSW solutions *contained* within the SuperKamiokande bands onto the x -axes, and taking their intersection. For instance, from the panels (a) and (d) one derives $\Delta\langle T\rangle/\langle T\rangle \simeq 1.8\text{--}4.5$ as the likely $\pm 1\sigma$ range for SNO (notice that the x -axis projections of the region L in panels (a) and (d) do not intersect). We can do an analogous exercise for panels 2(b,e) and 2(c,f). In summary, one obtains the following “ $\sim 1\sigma$ predictions” for SNO:

$$\text{SKam} \left\{ \begin{array}{l} \frac{N-D}{N+D} = 3.1 \pm 2.8\% \\ \frac{\Delta\langle T\rangle}{\langle T\rangle} = 0.95 \pm 0.73\% \end{array} \right. + \text{MSW} \implies \text{SNO} (\sim 1\sigma) \left\{ \begin{array}{l} \frac{N-D}{N+D} \simeq 0\text{--}6\% \\ \frac{\Delta\langle T\rangle}{\langle T\rangle} \simeq 1.8\text{--}4.5\% \\ \frac{CC/NC}{(CC/NC)_0} \simeq 15\text{--}50\% . \end{array} \right. \quad (3)$$

Of course, if the SuperKamiokande data in the above equation were used at $> 1\sigma$ level, then the predictive power for SNO would be rapidly lost, as a consequence of the relatively large experimental uncertainties.

If real SNO data were available, one could also draw in Fig. 2 “allowed vertical bands” whose intersection with the horizontal bands should then spot one of the two MSW solutions. The panels in Fig. 2 allow one to set easily the experimental accuracy needed to separate the MSW solutions between them and from the no oscillation point, using exclusively flux-independent information from SNO and SuperKamiokande. For instance, if the SuperKamiokande errors on $\Delta\langle T\rangle/\langle T\rangle$ and $N - D/N + D$ were reduced by a factor of two at

least, and if the corresponding SNO measurements could reach a similar fractional accuracy, then the S and L solutions would be easily distinguished, although with a statistical significance depending on the specific position of the data points. In particular, in the unlucky case of data points incidentally falling close to the no oscillation point (star), Figs. 2(a,b,d,e) show that the discriminative power would be reduced. In such cases (and in more general situations as well) the CC/NC measurement at SNO provides invaluable help, as evident from Figs. 2(c,f). In fact, with a prospective CC/NC uncertainty of a few percent, the two MSW solutions would be clearly separated from the no oscillation case (see also Ref. [17] for earlier studies). Therefore, using various combinations of flux-independent observables from SuperKamiokande and SNO, one should be able to separate the MSW solutions between them and from the no oscillation case. The experimental accuracy needed for such discrimination (which depends, to some extent, on the central value of the data) can be easily evaluated through Fig. 1(b) and Fig. 2 by drawing prospective error bands for SNO and SuperKamiokande.

In conclusion, we have shown the interplay between SuperKamiokande and SNO flux-independent observables within the MSW interpretation of the solar neutrino deficit. We have updated the small and large mixing angle MSW solutions by including the most recent flux-dependent data, and used such solutions as a guide for the flux-independent analysis. The SuperKamiokande energy spectrum and day-night asymmetry data have also been used to derive predictions for SNO. The estimated likely ranges for SNO are still rather large, but will steadily narrow as the SuperKamiokande uncertainties get reduced. Moreover, when the SNO experiment will also start operation, various combinations of SuperKamiokande and SNO flux-independent data will allow to spot either the large or the small mixing MSW solution, and to separate them from the no oscillation case. Our graphical representations show at glance the interplay between the two experiments, and allow to estimate *a priori* the experimental accuracy needed to separate the various cases with an assigned statistical significance.

One of us (E.L.) thanks the organizers of the Solar Neutrino Workshop “News about SNU’s” (Institute of Theoretical Physics, Santa Barbara, CA), where this work was initiated, for their kind hospitality and support.

TABLES

TABLE I. The five flux-independent observables considered in this work.

Experiment	Observable	Definition
SuperKamiokande	$(N - D)/(N + D)$	Night-day flux asymmetry
	$\Delta\langle T \rangle / \langle T \rangle$	Energy spectrum deviation
SNO	$(N - D)/(N + D)$	Night-day flux asymmetry
	$\Delta\langle T \rangle / \langle T \rangle$	Energy spectrum deviation
	CC/NC	Charged-to-neutral current ratio

TABLE II. Neutrino event rates measured by solar neutrino experiments, and corresponding predictions from the standard solar model [6]. The quoted errors are at 1σ .

Experiment	Ref.	Data \pm (stat.) \pm (syst.)	Theory [6]	Units
Homestake	[25]	$2.56 \pm 0.16 \pm 0.15$	$9.3^{+1.2}_{-1.4}$	SNU
Kamiokande	[2]	$2.80 \pm 0.19 \pm 0.33$	$6.62^{+0.93}_{-1.12}$	$10^6 \text{ cm}^{-2}\text{s}^{-1}$
SAGE	[26]	$69.9^{+8.5+3.9}_{-7.7-4.1}$	137^{+8}_{-7}	SNU
GALLEX	[27]	$76.4 \pm 6.3^{+4.5}_{-4.9}$	137^{+8}_{-7}	SNU
SuperKam.	[5]	$2.37^{+0.06+0.09}_{-0.05-0.06}$	$6.62^{+0.93}_{-1.12}$	$10^6 \text{ cm}^{-2}\text{s}^{-1}$

TABLE III. Energy spectrum of recoil electrons measured at SuperKamiokande (374 d). The numbers in columns 2–4 have been graphically reduced from the binned spectrum in [5,28] and represent: The ratio between data and theory (2nd column); the corresponding $\pm 1\sigma$ errors due to statistics plus uncorrelated systematics (3rd column) and to correlated systematics (4th column). Small asymmetries between upper and lower error bars have been neglected.

Bin energy range (MeV)	expt./theor. spectrum ratio	stat.+unc. syst. uncertainties	correl. syst. uncertainties
[6.5, 7]	0.327	± 0.030	± 0.004
[7, 7.5]	0.335	± 0.029	± 0.006
[7.5, 8]	0.402	± 0.030	± 0.008
[8, 8.5]	0.354	± 0.032	± 0.010
[8.5, 9]	0.304	± 0.032	± 0.012
[9, 9.5]	0.345	± 0.036	± 0.014
[9.5, 10]	0.382	± 0.042	± 0.016
[10, 10.5]	0.367	± 0.045	± 0.017
[10.5, 11]	0.308	± 0.045	± 0.023
[11, 11.5]	0.377	± 0.055	± 0.026
[11.5, 12]	0.360	± 0.063	± 0.036
[12, 12.5]	0.404	± 0.077	± 0.042
[12.5, 13]	0.390	± 0.087	± 0.046
[13, 13.5]	0.504	± 0.119	± 0.063
[13.5, 14]	0.490	± 0.146	± 0.101
[14, 20]	0.562	± 0.154	± 0.114

REFERENCES

- [1] R. Davis (Homestake Collaboration), *Prog. Part. Nucl. Phys.* **32**, 13 (1994).
- [2] Y. Fukuda *et al.* (Kamiokande Collaboration), *Phys. Rev. Lett.* **77**, 1683 (1996).
- [3] J. N. Abdurashitov *et al.* (SAGE Collaboration), *Phys. Rev. Lett.* **77**, 4708 (1996).
- [4] W. Hampel *et al.* (GALLEX Collaboration), **288**, 384 (1996).
- [5] Y. Totsuka (SuperKamiokande Collaboration), in the Proceedings of the 35th International School of Subnuclear Physics (Erice, Italy, 1997), to appear.
- [6] J. N. Bahcall and M. H. Pinsonneault, *Rev. Mod. Phys.* **67**, 781 (1995).
- [7] V. Castellani, S. Degl’Innocenti, G. Fiorentini, M. Lissia, and B. Ricci, *Phys. Rept.* **281**, 309 (1997).
- [8] J. N. Bahcall, *Neutrino Astrophysics* (Cambridge University Press, Cambridge, England, 1989).
- [9] L. Wolfenstein, *Phys. Rev. D* **17**, 2369 (1978); S. P. Mikheyev and A. Yu. Smirnov, *Yad. Fiz.* **42**, 1441 (1985) [*Sov. J. Nucl. Phys.* **42**, 913 (1986)]; *Nuovo Cimento C* **9**, 17 (1986).
- [10] E. Lisi and D. Montanino, *Phys. Rev. D* **56**, 1792 (1997).
- [11] G. L. Fogli, E. Lisi and D. Montanino, University of Bari Report No. BARI-TH/284-97, hep-ph/9709473, to appear in *Astropart. Phys.*
- [12] N. Hata and P. Langacker, *Phys. Rev. D* **56**, 6107 (1997).
- [13] J. N. Bahcall and P. I. Krastev, *Phys. Rev. C* **56**, 2839 (1997).
- [14] G. L. Fogli and E. Lisi, *Astropart. Phys.* **3**, 185 (1995).
- [15] A. B. McDonald (SNO Collaboration), in *TAUP ’95*, Proceedings of the 4th International Conference on Theoretical and Phenomenological Aspects of Underground Physics, Toledo, Spain, 1995, ed. by A. Morales, J. Morales, and J. A. Villar, [*Nucl. Phys. B* **48** (Proc. Suppl.)], p. 357; M. E. Moorhead, *ibidem*, p. 378.
- [16] J. N. Bahcall, P. I. Krastev, and E. Lisi, *Phys. Rev. C* **55**, 494 (1997).
- [17] J. N. Bahcall and E. Lisi, *Phys. Rev. D* **54**, 5417 (1996).
- [18] W. Kwong and S. P. Rosen, *Phys. Rev. D* **54**, 2043 (1996).
- [19] M. Nakahata, in *P4 ’97*, Proceedings of the APCPT Pacific Particle Physics Phenomenology Conference, (Seoul, Korea, 1997); also available at the URL <http://www-sk.icrr.u-tokyo.ac.jp/doc/sk/pub/~>.
- [20] K. Inoue, in *TAUP ’97*, Proceedings of the 5th International Workshop on Topics in AstroParticle and Underground Physics (Gran Sasso, Italy, 1997), to appear in *Nucl. Phys. B* (Proc. Suppl.); also available at the same URL as ref. [19].
- [21] Y. Suzuki, in *Neutrinos in Astro, Particle and Nuclear Physics*, Proceedings of the 19th International School of Nuclear Physics (Erice, Italy, 1997), to appear; also available at the same URL as ref. [19].
- [22] Y. Itow, in the Proceedings of the Topical Conference “Physics of Leptons,” SLAC Summer Institute 1997; (Stanford, CA, 1997), to appear; also available at the same URL as ref. [19].
- [23] H. Sobel, in the Proceedings of the Aspen Winter Conference on Particle Physics: Frontiers in Particle Physics (Aspen, CO, 1998), to appear.
- [24] R. Svoboda, in *News about SNU’s*, International Workshop on Solar Neutrinos (Institute

- of Theoretical Physics, Santa Barbara, CA, 1997). Proceedings available at the URL <http://www.itp.ucsb.edu/online/snu> .
- [25] K. Lande (Homestake Collaboration), in $\nu 4$, Proceedings of the 4th International Solar Neutrino Conference, Heidelberg, Germany, 1997, ed by W. Hampel (Max Planck Institute, Heidelberg, 1998), p. 85.
- [26] V. N. Gavrin (SAGE Collaboration), in *News about SNU's* [24].
- [27] W. Hampel (GALLEX Collaboration), in *News about SNU's* [24].
- [28] We thank R. Svoboda for providing us with a figure of the experimental electron spectrum with separated error components (correlated systematics and statistical uncertainties plus uncorrelated systematics).
- [29] J. N. Bahcall, E. Lisi, D. E. Alburger, L. De Braekeleer, S. J. Freedman, and J. Napolitano, Phys. Rev. C **54**, 411 (1996).

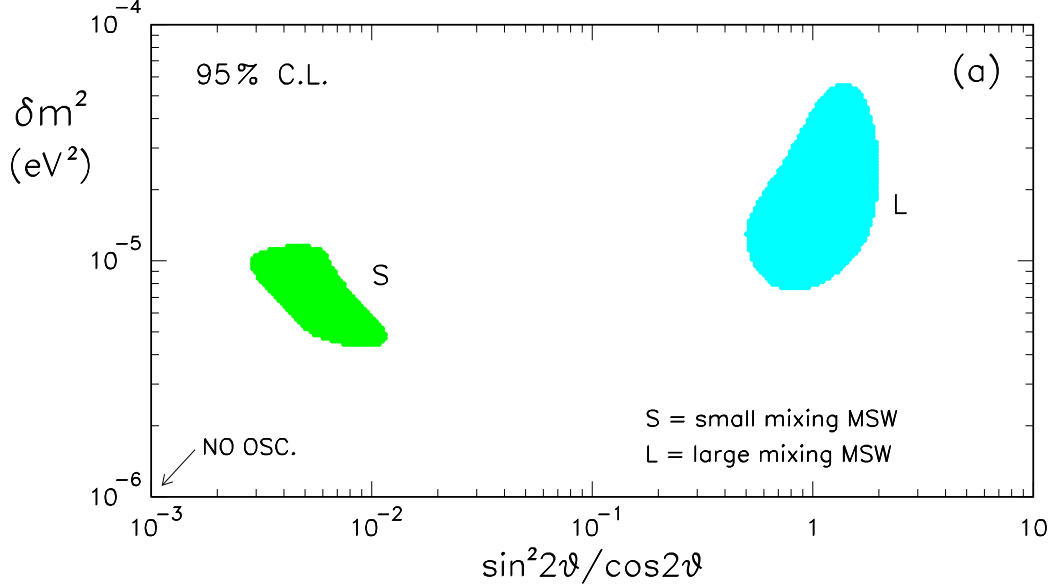
FIGURES

FIG. 1. Summary of flux dependent and independent information on the MSW solutions. (a) MSW fit to the total neutrino rates measured by SuperKamiokande (374 days), Kamiokande, Homestake, SAGE and GALLEX (see Table I), showing the small mixing (S) and large mixing (L) solutions at 95% C.L. in the neutrino mass-mixing plane. (b) Map of the S and L solutions in the plane spanned by two flux-independent SuperKamiokande observables: the day-night asymmetry $N - D/N + D$ and the mean kinetic energy deviation $\Delta\langle T\rangle/\langle T\rangle$. Also shown are the experimental data after 306 and 374 days of operation, and the “no oscillation” point. See the text for details.

FIG. 2. Relation between flux-independent observables at SuperKamiokande ($\frac{N-D}{N+D}$ and $\frac{\Delta\langle T\rangle}{\langle T\rangle}$) and at SNO ($\frac{N-D}{N+D}$, $\frac{\Delta\langle T\rangle}{\langle T\rangle}$, and $\frac{CC}{NC}$). The S and L solutions of Fig. 1(a) are mapped onto each plane, together with the “no oscillation” point (star). The horizontal bands represent the $\pm 1\sigma$ data from SuperKamiokande (374 days). The MSW predictions for SNO (at $\sim 1\sigma$ level) can be obtained by projecting the part of the MSW solutions contained within such bands onto the x -axes, and taking their intersection.

FLUX – DEPENDENT INFORMATION

[SKam(374 d) + Kam + Cl + Ga total neutrino rates]



FLUX – INDEPENDENT INFORMATION

[SuperKamiokande day–night and energy spectra]

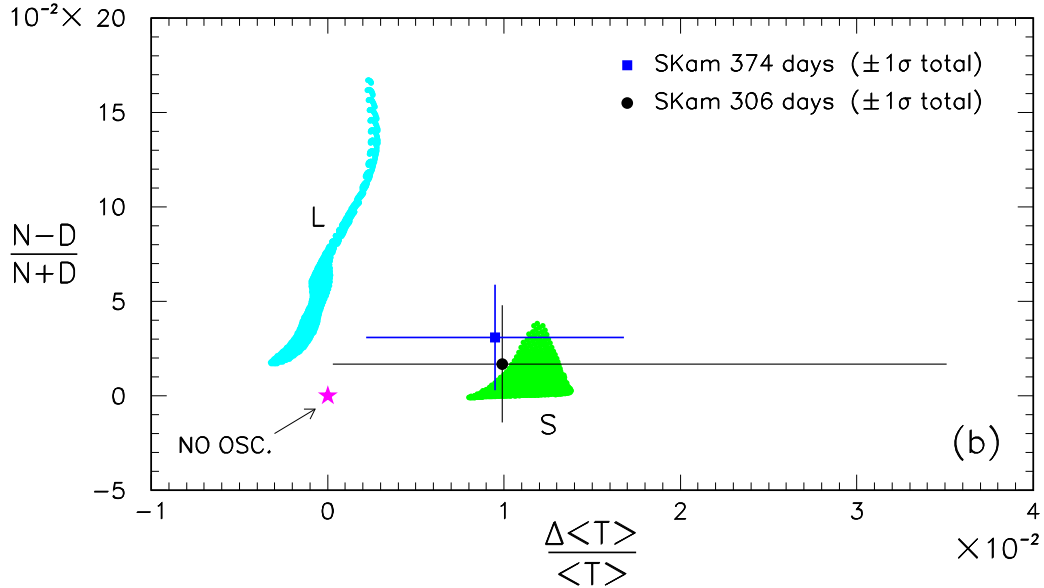


FIG. 1. Summary of flux dependent and independent information on the MSW solutions. (a) MSW fit to the total neutrino rates measured by SuperKamiokande (374 days), Kamiokande, Homestake, SAGE and GALLEX (see Table I), showing the small mixing (S) and large mixing (L) solutions at 95% C.L. in the neutrino mass-mixing plane. (b) Map of the S and L solutions in the plane spanned by two flux-independent SuperKamiokande observables: the day-night asymmetry $N - D/N + D$ and the mean kinetic energy deviation $\Delta\langle T \rangle/\langle T \rangle$. Also shown are the experimental data after 306 and 374 days of operation, and the “no oscillation” point. See the text for details.

Relation between SKam and SNO flux-independent observables

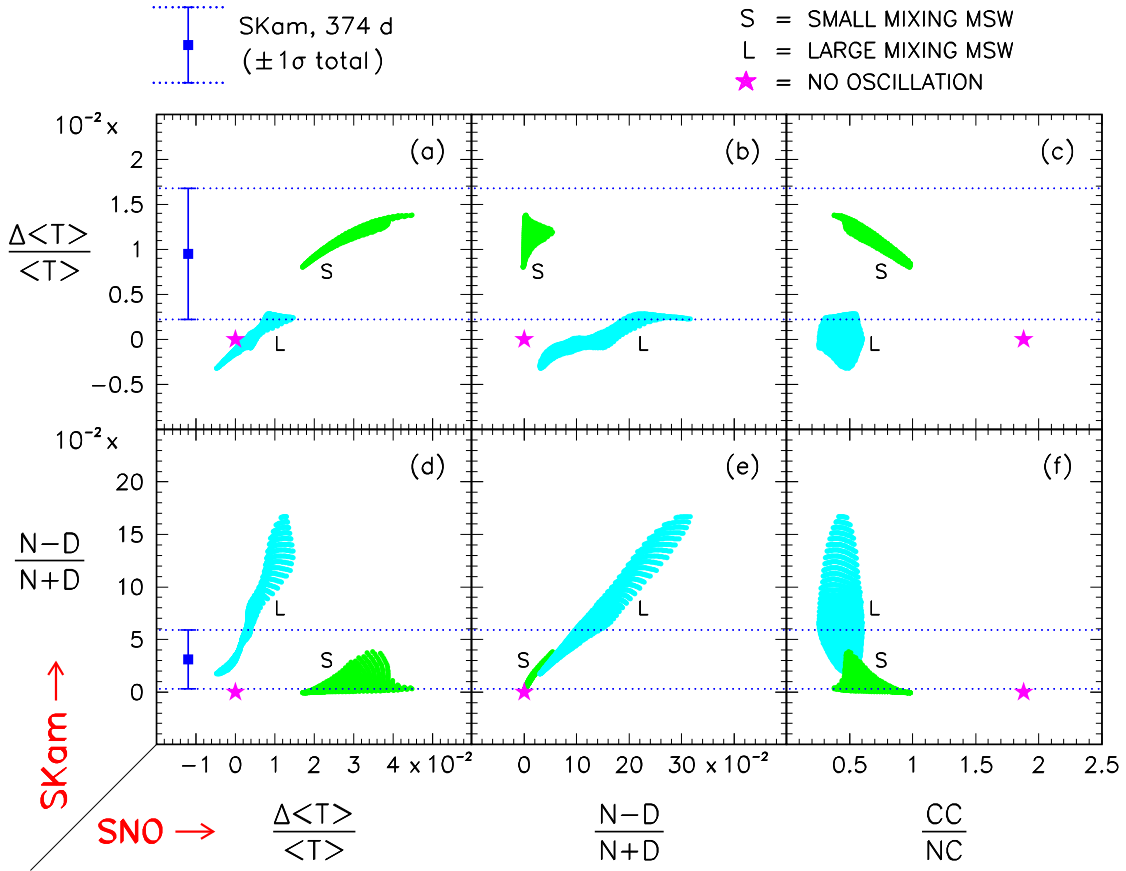


FIG. 2. Relation between flux-independent observables at SuperKamiokande ($\frac{N-D}{N+D}$ and $\frac{\Delta\langle T \rangle}{\langle T \rangle}$) and at SNO ($\frac{N-D}{N+D}$, $\frac{\Delta\langle T \rangle}{\langle T \rangle}$, and $\frac{CC}{NC}$). The S and L solutions of Fig. 1(a) are mapped onto each plane, together with the "no oscillation" point (star). The horizontal bands represent the $\pm 1\sigma$ data from SuperKamiokande (374 days). The MSW predictions for SNO (at $\sim 1\sigma$ level) can be obtained by projecting the part of the MSW solutions contained within such bands onto the x -axes, and taking their intersection.